Sensors and Materials, Vol. 35, No. # (2023) 1–##
MYU Tokyo

S & M ####

Experimental Analyses of Aerodynamic Force Generation and Wing Motion Associated with a Single-motor-driven Butterfly-inspired Flapping-wing Robot

Shogo Miyasaka,[1] Chang-kwon Kang,[2] and Hikaru Aono[1*]

[1]Shinshu University, 3-15-1, Tokida, Ueda 386-8567, Japan
[2]The University of Alabama in Huntsville, Huntsville, Alabama 35899, U.S.A.

(Received February 3, 2023; accepted March 7, 2023)

Keywords: flapping wing, butterfly-inspired aerial robot, simultaneous measurement, elastic band, single motor

The fascinating flight traits of butterflies, such as low wing loading, low flapping frequency, and the ability for long-distance flight, have intrigued scientists and engineers. To study these mechanisms, a 2.7 g butterfly-inspired flapping-wing micro air vehicle (FWMAV) was developed using a combination of a single motor, elastic bands, a driving shaft, shape optimization, and a butterfly-like wing planform. During tethered experiments, aerodynamic forces and wing motions were simultaneously measured to understand the aerodynamics of the butterfly-inspired FWMAV. The results show that the ranges of resultant flapping and lead-lag motion of the wing of the robot were within those of real butterflies during the first stroke. The lift varied with the flapping motion and was sufficient for flight but averaged to zero over one flapping cycle because the opposite direction of lift was generated during the upstroke. These findings indicate that the modulation of the resulting aerodynamic force direction due to the control of the stroke plane angle per stroke plays a crucial role in the flights of butterflies and butterfly-inspired FWMAVs.

1. Introduction

The functions of animals have been a topic of interest for many scientists, and the development of bio-inspired robots has been on ongoing field of study for a long time.[1–3] Flapping-wing micro air vehicles (FWMAVs)[4,5] were inspired by the movements and functions of the wings and bodies of flying insects and birds.[6,7] It is expected that FWMAVs will be used as an element of observation and information gathering systems for unknown and hazardous environments. Owing to advances in manufacturing technology and a better understanding of fundamental aerodynamic mechanisms in flapping wing aerodynamics, several types of bio-inspired FWMAVs have demonstrated controlled flight in indoor[8,9] and outdoor environments.[10–14]

*Corresponding author: e-mail: aono@shinshu-u.ac.jp
https://doi.org/10.18494/SAM4343

ISSN 0914-4935
https://myukk.org/

Among many biological flyers, we focus on the flights of butterflies and a butterfly-inspired FWMAV in this study. One of the motivations comes from the observations that species of butterflies (e.g., chestnut tiger and monarch butterfly) migrate over long distances across continents[15,16] and fly at high altitudes.[17] Furthermore, the flights of butterflies are characterized by a low wing loading and a low flapping frequency in comparison with those of other insects. Moreover, butterflies use the change in stroke plane angle between the downstroke and the upstroke to modulate the direction of aerodynamic forces and torques, whereas most flying insects and birds change the direction of lift force by changing the pitching angle of their wings.

Fujikawa *et al.* built a 1 g butterfly-style flapping robot based on a rubber-band-driven crank mechanism.[18] Using this robot, they looked at the effects of the relative position of the center of lift on the resulting flight behavior.[18] Subsequently, a simple slide-crank mechanism incorporating flexible links was added to the robot to achieve both flapping and lead-lag motions,[19] and the glide characteristics and attitude stability of the modified robot were investigated.[20] At the same time, Tanaka and Shimoyama built a 0.39 g butterfly-type ornithopter based on the rubber-band-driven crank mechanism.[21] They investigated an inactive feathering or feedback control of the wing motion that would be a possible mechanism behind the stable forward flight of swallowtail butterflies.[21] Rubber actuator models are simple structures and exhibited a high power/mass ratio even though the flight distance is very short because the actuator only flaps the wings a couple of times because the twisting torque quickly decays.

To increase the flight distance and analysis area, Fujikawa and Kikuchi developed a 0.9 g butterfly-style flapping wing robot without a battery based on a single motor and elastic bands.[22] A posture control mechanism of the robot was tested by varying the ratio of downstroke and upstroke times,[22] and the effects of flapping motion on gliding performance were measured.[23] There were also 55 g butterfly-like flapping robots with tenfold enlarged wings,[8] which were able to fly. However, the wing motion and the trajectory of the center of gravity of the robots were different from those of actual butterflies. The main reason was that the movements of the wings and bodies of butterflies were more challenging to reproduce using mechanical parts than those of other insects owing to the considerable interaction between the wing and the body.[24,25]

Previous studies[8,14,18–25] have shown progress in developing butterfly-inspired FWMAVs and understanding butterfly flight mechanisms, but the connection between aerodynamic force and wing and body motions in robots remains unclear. In this study, we aim to shed light on the issue by constructing a single-motor-driven butterfly-inspired FWMAV and investigating the relationship between wing motion and aerodynamic force generation through simultaneous measurements under tethered conditions. The aerodynamic forces produced by the FWMAV are tracked using a force transducer, and wing motion is captured in real time by two high-speed cameras.

2. Materials and Methods

2.1 Butterfly-inspired flapping wing robot design

Figure 1 illustrates the design of the butterfly-inspired FWMAV, named robo-butterfly Shinshu, with a bird's eye view of the structure and mechanism of its wing actuation, and a detailed view of the separated components of the wing planform. The robo-butterfly Shinshu has a wingtip-to-wingtip length of 175 mm, a forewing span of 80 mm, and a hindwing span of 43 mm, similar to previous studies.[18,19,22,23] Its wing is made of a 12.5 μm Kapton film reinforced with 0.3 mm carbon rods serving as veins. The design of the wings was based on the dynamic similarity[6] by matching the Reynolds numbers, reduced frequency, and angle of attack. In addition, the aspect ratio, wing loading, and flapping frequency were chosen so that these were close to the range of real butterflies.[26,27] Moreover, the effects of the vein structures of the real butterfly wings were not considered and are one of our on-going research topics.[28,29] The body frame is constructed using an acrylic resin (AR-M2), designed with CAD software (Fusion360, Autodesk), and fabricated using a 3D printer (AGILISTA-3200, Keyence). The motor box geometry was optimized to reduce weight. The robot weighs 2.70 g (W = 0.026 N), including a pinion gear (GW338, DIDEL), a spur gear (G336L, DIDEL), a motor (MK04-10, DIDEL), and a Li-Po battery (FX10S, 10 mAh, 15C/150 mA), and has a wing loading of 3.63 N/m^2 with a total wing area of 7312 mm^2, comparable to that of real butterflies.[16–19,26,27] Figure 2 shows the mass distribution of the robo-butterfly Shinshu. Figure 1(b) shows the motion of the

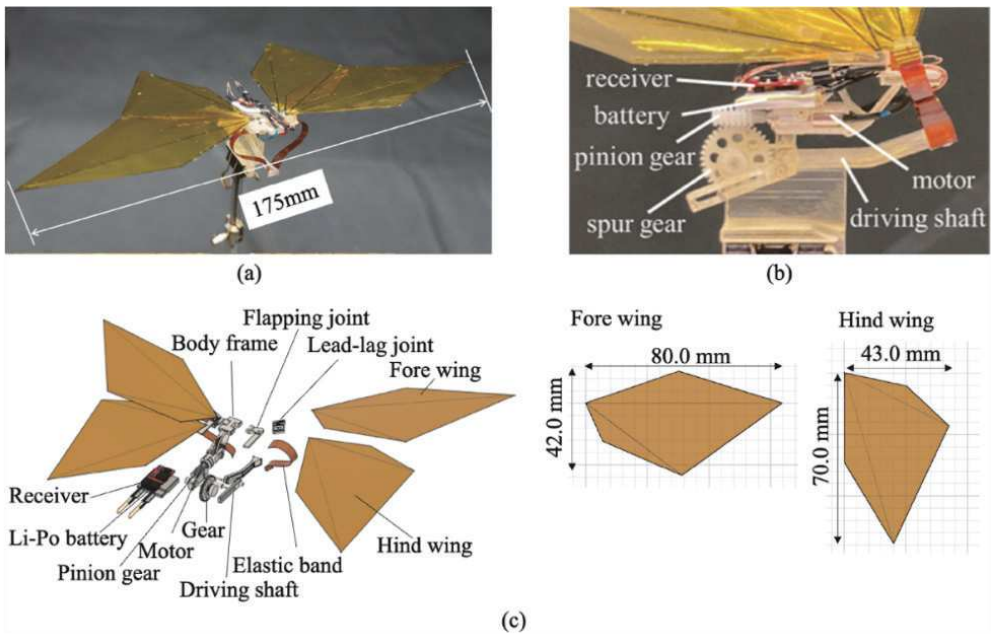

Fig. 1. (Color online) (a) Overview of the robo-butterfly Shinshu, a butterfly-inspired FWMAV. (b) Magnified view of the wing actuation mechanism. (c) Exploded view of the main structures of the robo-butterfly Shinshu and wing planform of fore- and hindwings.

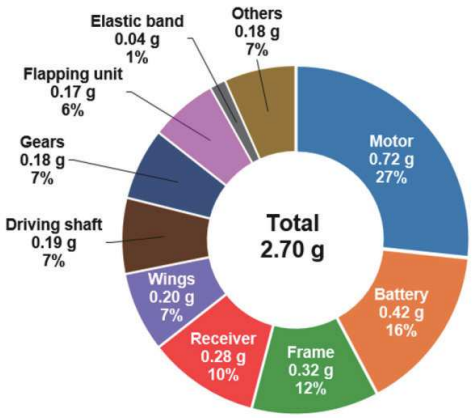

Fig. 2. (Color online) Mass breakdown of the robo-butterfly Shinshu.

motor being converted to a reciprocal flapping motion through a crank mechanism. The wing also undergoes a lead-lag motion through an elastic band connected to the drive shaft, similar to previous studies.[19,21] The elastic band is made of a 125-μm-thick Kapton film and is 4 mm wide and 33 mm long. Its shape and attachment were determined through trial and error. The robo-butterfly Shinshu's design emphasizes a flapping motion with a lead lag, a forward center of lift, and a large flapping amplitude, based on the observations of real butterflies[19] and previous studies using the robot.[21,22] The motor and gear unit are located at the rear of the body to place the center of gravity near the rear. The pitch motion of the body is not included in the design of the model presented in this study.

The referenced flapping and lead-lag angle histories of a real butterfly were those of a swallowtail butterfly (*Paplio xuthus*) during the first stroke reported in a previous study.[19] The range of the flapping angle was from −60 to 80° and the range of the lead-lag angle was from −5 to 15°. The frequency of the lead-lag angle was twice the flapping frequency.

2.2 Measurement of aerodynamic force and wing motion

Figure 3 shows that the experimental setup used to investigate the relationship between the wing motion and aerodynamic force generation of the robo-butterfly Shinshu involved the use of a six-axis force transducer (ATI Nano17 Ti, ATI Industrial Automation), a data acquisition device (USB-6341, National Instruments), a PC, and two high-speed cameras (HAS-DX, Ditect). The force transducer was used to measure aerodynamic force and torque and was connected to a computer with a sampling frequency of 2000 Hz. The wing motion was recorded using the two high-speed cameras with a sampling rate of 2000 frames per second, and a light source (PFBR-150SW-MN, CCS) was used to improve the quality of the recorded video. The eight markers on the right wing were tracked and analyzed using an in-house photogrammetric deformation measurement program,[30] and the 3D coordinates of all markers were recorded and analyzed. An external power supply (PW8-3AQP, Texio) provided stable electrical power to the robo-

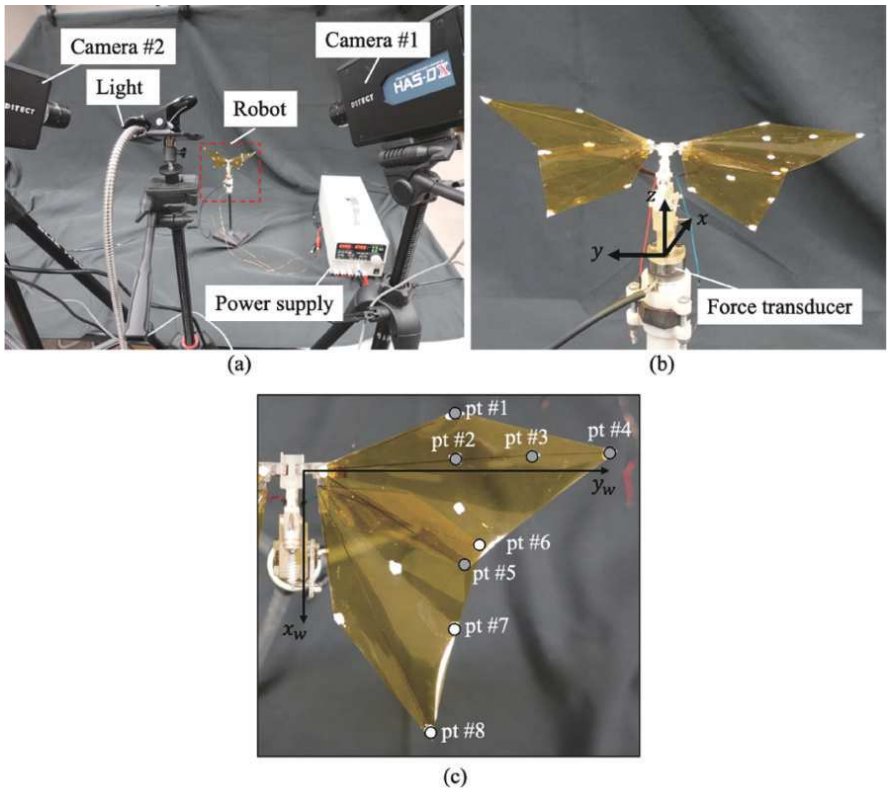

Fig. 3. (Color online) (a) Experimental setup of the simultaneous lift and wing motion measurement, (b) magnified view of the robot, and (c) tracking markers on the fore- and hindwings.

butterfly Shinshu with a voltage of 4.2 V and a current of 0.15 A. This input condition is the same as that of a Li-Po battery that will be installed. A low-pass filter with a cutoff frequency of four times the flapping frequency was applied. Thrust (F_x) and lift (F_z) were defined as the forces in the x- and z-axis directions, respectively, in the coordinate system.

Figure 4 shows the wing coordinate system used to analyze the wing motion of the robo-butterfly Shinshu. The lead-lag angle (θ) and flapping angle (ϕ) are defined in Fig. 4. The stroke plane is along the z_w-axis. Flapping frequency was computed by the frequency analysis of the time history of the flapping angle. The data was recorded for 0.5845 s, which included three flapping cycles. Cycle-averaged data were computed on the basis of three flapping motions (denoted by an upper bar symbol). The cycle-averaged lift and thrust are discussed on the basis of this information.

3. Results and Discussion

Figure 5 shows the time histories of aerodynamic forces and wing angles at the tip of the forewing [i.e., pt #4 in Fig. 3(c)]. The flapping frequency was 7.0 Hz and the period of flapping motion (T) was 0.1429 s. Results from the switching on the robo-butterfly Shinshu ($t/T = 0$) to around $t/T = 0.9$ are not considered in the discussion.

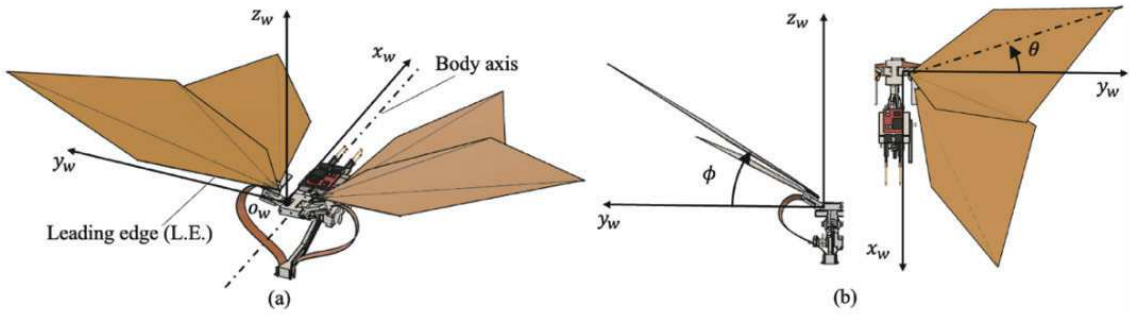

Fig. 4. (Color online) (a) Schematic diagrams of wing coordinate system and (b) definitions of flapping angle and lead-lag angle θ.

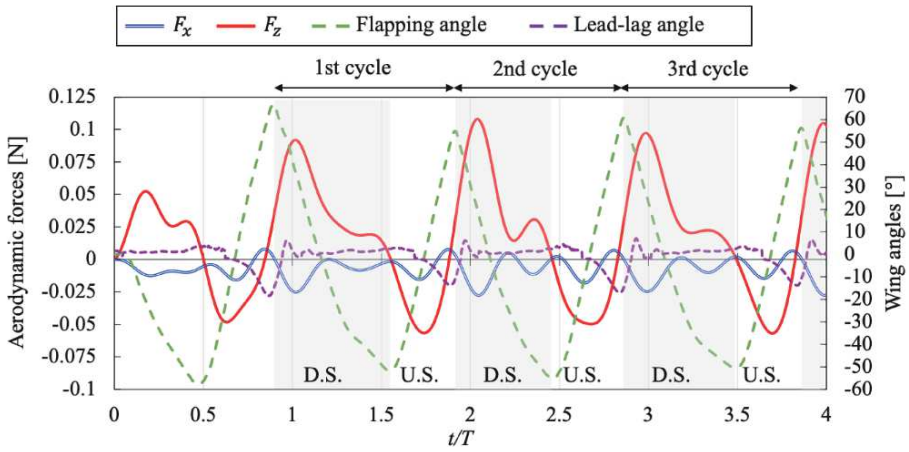

Fig. 5. (Color online) Time histories of aerodynamic forces (F_x and F_z) and wing angles at the wing tip (ϕ and θ). T, D.S., and U.S. denote the period of flapping motion, downstroke, and upstroke, respectively.

The lift (F_z) and thrust (F_x) change as the wing angles change. During the downstroke, positive lift is generated, whereas negative lift is produced during the upstroke. The half stroke average data shown in Table 1 indicates that the lift generated during the downstroke is sufficient to offset the weight of the robo-butterfly Shinshu. Although the half stroke average lift is negative, its magnitude is larger than the weight of the robo-butterfly Shinshu. The lift has two peaks, with the first and largest peak appearing in the early downstroke, and the second near the end of the downstroke. Negative thrust is generated during most of the stroke, and both cycle and half stroke average thrusts are negative, implying that drag is generated. The magnitude of lift is much larger than that of thrust owing to the appearance of a large angle of attack of the wing during both strokes (the average values are approximately 98 and 80° over the downstroke and upstroke, respectively).

Figure 6 shows a comparison of the time histories of the flapping and lead-lag angles of the wing between the robo-butterfly Shinshu and a real butterfly in the first stroke.[19] The ratio of the downstroke and upstroke was around 60:40. The ranges of the flapping and lead-lag angles

Table 1
Averaged aerodynamic force data and ratio of aerodynamic force and weight. W denotes the weight of the robo-butterfly Shinshu.

	Cycle average	Downstroke average	Upstroke average
$\overline{F_x}$	−0.013 N	−0.008 N	−0.005 N
$\lvert\overline{F_x}/W\rvert$	0.49	0.30	0.19
$\overline{F_z}$	0.007 N	0.041 N	−0.034 N
$\lvert\overline{F_z}/W\rvert$	0.26	1.55	1.28

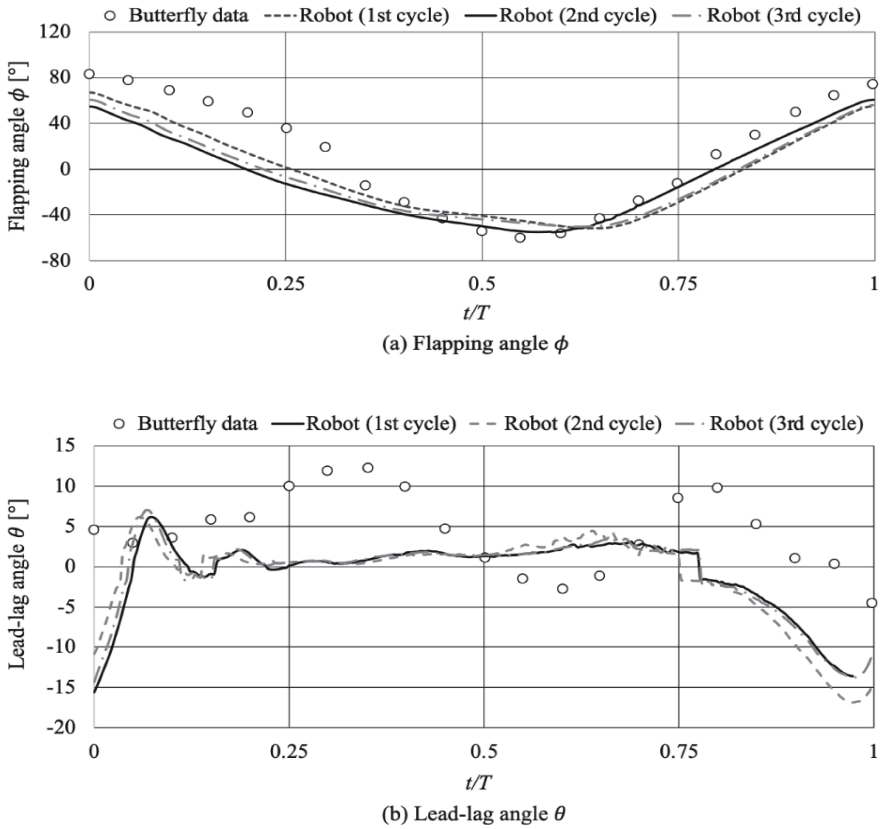

Fig. 6. Comparison of time histories of (a) flapping angle (ϕ) and (b) lead-lag angle (θ) of the forewing between the robo-butterfly Shinshu and a real butterfly.[19] T denotes the period of flapping motion.

of the robo-butterfly Shinshu are comparable to those of a real butterfly.[19] The time histories of the flapping angle of the robo-butterfly Shinshu are in close agreement with the data of real butterflies. However, further improvement of the time histories of the lead-lag angle of the robo-butterfly Shinshu is required. The lead-lag angle is almost constant during the downstroke but decreases during the upstroke. Furthermore, the rates of changes in flapping and lead-lag angle also change as seen in Figs. 5 and 6. The rate of change in flapping angle changes at the end of the downstroke, whereas the rate of change in lead-lag angle changes at the stroke reversal from

the upstroke to the downstroke. This is likely due to the stretch and twist of the elastic band attached to the driving shift. The Reynolds number, reduced frequency, and aspect ratio of the robo-butterfly Shinshu were 5738, 0.43, and 4.19, respectively, which are within the range of real butterflies.[17,19,26,27] The angle of attack for the robo-butterfly Shinshu is purely due to the wing deformation (i.e., passive pitch). When the resulting angle of attack is close to the butterfly motion, dynamic similarity[6] is achieved such that the flow structures around the wings are similar to those reported in previous studies.[26,27]

Figure 7 shows the time histories of the flapping and lead-lag angles reconstructed from the positions of markers on the fore- and hindwings shown in Fig. 3(c) (see the supplementary video). The time histories of flapping angles of all points indicated that the fore- and hindwings flapped with insignificant bending deformation. Also, the time-varying lead-lag angle of all points indicated that the motion of the forewing resembled a rigid rotation without notable deformations. Results implicate that the wings of the robo-butterfly Shinshu acted as a very thin rigid-like flat plate.

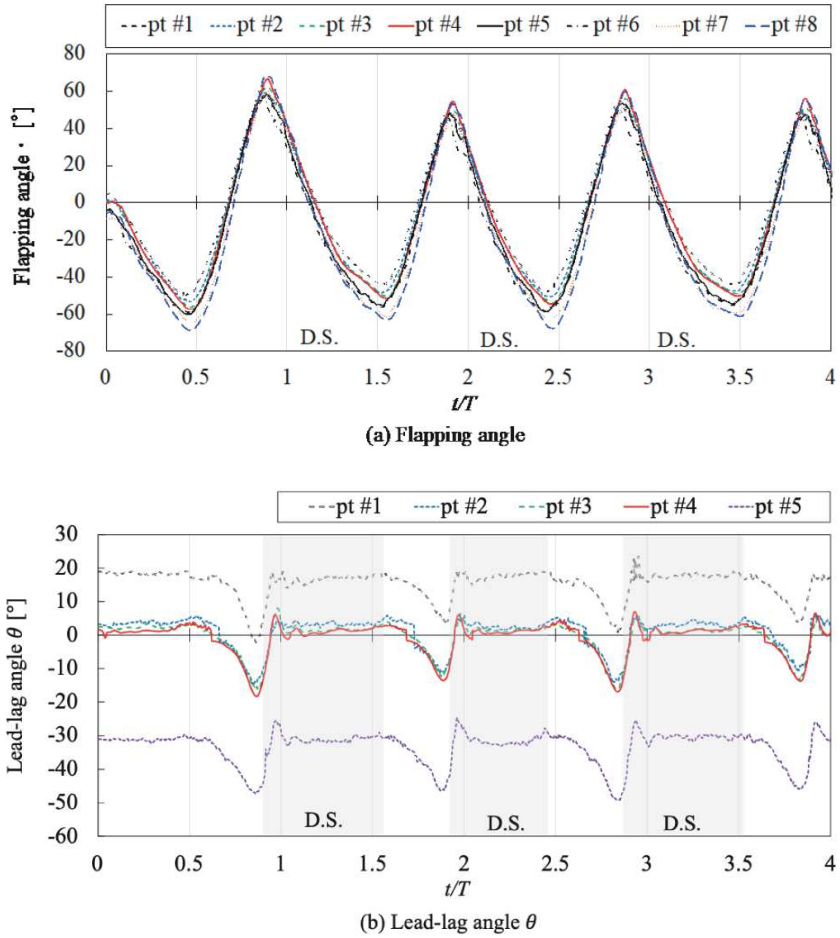

Fig. 7. (Color online) Time histories of (a) flapping angle (ϕ) of fore- and hindwings and (b) lead-lag angle (θ) of the forewing. T and D.S. denote the period of flapping motion and downstroke, respectively.

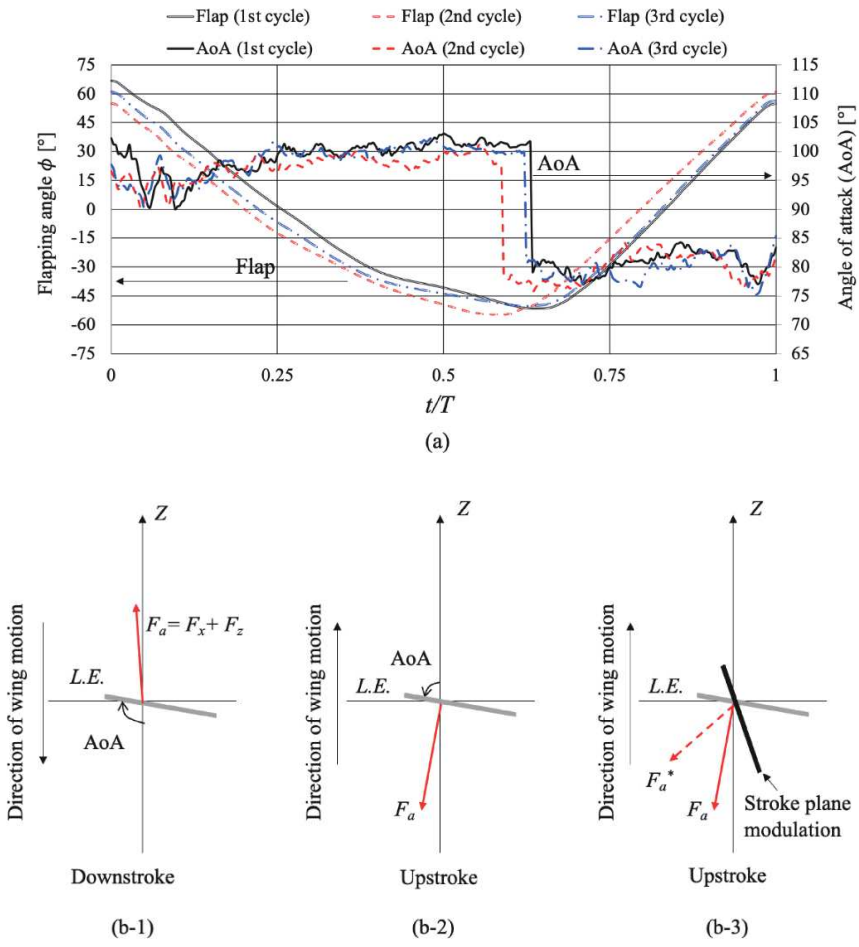

Fig. 8. (Color online) (a) Time histories of flapping angle and local sectional angle of attack of forewing and (b-1, b-2) schematic diagrams of resulting aerodynamic force acting on the wing and the angle of attack over the stroke. (b-3) Illustration of effects of stroke plane angle modulation on the resultant aerodynamic force acting on the wing during the upstroke.

On the basis of the 3D coordinate data of two points of the forewing (i.e., pt #1 and #4), the local sectional angle of attack (AoA) was calculated. Figure 8 shows the time histories of the local sectional AoA and flapping angle of the forewing and illustrates a schematic diagram of the resulting aerodynamic force acting on the wing section. Looking at Figs. 5 and 8, the maximum positive lift generation occurred when the local sectional AoA of the forewing was close to 90°. The AoA of the forewing remained constant in most of the strokes. The large local sectional AoA implies flow separation from the leading and trailing edges. As such, it is likely that the leading and trailing-edge vortices during both strokes are generated, resulting in the insect unsteady flow mechanisms. As explained in Fig. 8(b), the modulation of lift force during the upstroke appeared promising for less negative lift generation in one flapping cycle and the reproduction of butterfly-like body motion due to the change in the direction of the resulting aerodynamic forces acting on the wing.

4. Conclusions

In this study, we developed a 2.7 g butterfly-inspired FWMAV with an on-board battery, named the robo-butterfly Shinshu. The flapping and lead-lag motions of the wings were generated using an elastic band, a single motor, a driving shaft, and flapping/lead-lag joints. The results of the simultaneous measurements of wing motion and aerodynamic forces under the tethered condition showed that the robo-butterfly Shinshu flapped at a rate of 7.0 Hz, generated lift during the downstroke, which is large enough to offset its own weight, and had a cycle-averaged lift close to zero. Results suggest the importance of the modulation of the stroke plane angle to adjust the direction of the resulting aerodynamic force generated by the wings during the flight of butterflies and butterfly-inspired FWMAVs. The current experiments of the tethered robo-butterfly Shinshu did not include the body pitching motion. Future work will focus on developing a rotation mechanism of the stroke plane for the robo-butterfly Shinshu to demonstrate stable forward flight and reproduce the movements observed in real butterflies.

Acknowledgments

This work was partly supported by the Japan Society for the Promotion of Science KAKENHI Grant Number JP22H01397. CK was partly supported by the National Science Foundation (grant number CMMI-1761618). The authors thank Dr. Taku Nonomura, Dr. Keisuke Asai, Dr. Yuta Ozawa, and Mr. Kento Akama for their support in the measurement of wing deformation.

References

1 J. F. V. Vincent, O. A. Bogatyreva, N. R. Bogatyrev, A. Bowyer, and A.-K. Pahl: J. R. Soc. Interface **3** (2006) 471. https://doi.org/10.1098/rsif.2006.0127
2 Y. Bar-Cohen: Bioinspiration Biomimetics **1** (2006) P1. https://doi.org/10.1088/1748-3182/1/1/P01
3 B. Bhushan: Phil. Trans. R. Soc. A **367** (2009) 1445. https://doi.org/10.1098/rsta.2009.0011
4 H. V. Phan and H. C. Park: Prog. Aerosp. Sci. **111** (2019) 1. https://doi.org/10.1016/j.paerosci.2019.100573
5 G. de Croon: Sci. Rob. **5** (2020) 1. https://doi.org/10.1126/scirobotics.abd0233
6 W. Shyy, H. Aono, C.-K. Kang, and H. Liu: An Introduction to Flapping Wing Aerodynamics (Cambridge University Press, Cambridge, 2020) 1st ed., pp. 1–258.
7 D. D. Chin and D. Lentink: J. Exp. Biol. **219** (2016) 920. https://doi.org/10.1242/jeb.042317
8 H. Huang, W. He, Z. Chen, T. Niu, and Q. Fu: Biomimetic Intell. Rob. **2** (2022) 1. https://doi.org/10.1016/j.birob.2022.100076
9 H. Nagai, K. Nakamura, K. Fujita, I. Tanaka, S. Nagasaki, Y. Kinjo, S. Kuwazono, and M. Murozono: Sens. Mater. **33** (2021) 859. https://doi.org/10.18494/SAM.2021.3222
10 M. Keennon, K. Klingebiel, H. Won, and A. Andriukov: Proc. 50th AIAA Aerospace Sciences Meeting including the New Horizons Forum and Aerospace Exposition (AIAA, 2012) 1–24.
11 M. Karasek, F. T. Muijres, C. de Wagter, B. D. W. Remes, and G. C. H. E. de Croon: Science **361** (2018) 1089. https://doi.org/10.1126/science.aat0350
12 T. Zhang, F. Fei, and X. Deng: IEEE Rob. Autom. Lett. **5** (2020) 4194. https://doi.org/10.1109/LRA.2020.2974717
13 H. V. Phan, S. Aurecianus, T. K. L. Au, T. Kang, and H. C. Park: IEEE Rob. Autom. Lett. **5** (2020) 5059. https://doi.org/10.1109/LRA.2020.3005127
14 FESTO eMotionButterflies: https://www.festo.com/us/en/e/about-festo/research-and-development/bionic-learning-network/highlights-from-2015-to-2017/emotionbutterflies-id_33454/ (accessed March 2023).
15 L. P. Brower: J. Lepid. Soc. **49** (1995) 304.
16 C. Le Roy, V. Debat, and V. Llaurens: Biol. Rev. **94** (2019) 1261. https://doi.org/10.1111/brv.12500

17 M. K. Sridhar, C.-K. Kang, D. B. Landrum, H. Aono, S. L. Mathis, and T. Lee: Bioinspiration Biomimetics **16** (2021) 1. https://doi.org/10.1088/1748-3190/abe108
18 T. Fujikawa, Y. Sato, Y. Makata, T. Yamashita, and K. Kikuchi: Proc. 2008 IEEE Int. Conf. Robotics and Biomimetics (IEEE, 2009) 216–221.
19 T. Fujikawa, Y. Sato, T. Yamashita, and K. Kikuchi: Proc. 2010 World Automation Congress (IEEE, 2010) 16.
20 A. Hosoi, S. Sato, Y. Ozawa, K. Kikuchi, and T. Fujikawa: J. Jpn. Soc. Design Eng. **54** (2019) 265. https://doi.org/10.14953/jjsde.2018.2796
21 H. Tanaka and I. Shimoyama: Bioinspiration Biomimetics **5** (2010) 1. https://doi.org/10.1088/1748-3182/5/2/026003
22 T. Fujikawa and K. Kikuchi: J. Jpn. Soc. Design Eng. **54** (2019) 199. https://doi.org/10.14953/jjsde.2018.2797
23 M. Kawasaki, T. Fujikawa, K. Kikuchi: Proc. 5th Int. Conf. Design Engineering and Science: ICDES2020 (ICDES, 2020) 289–295.
24 C.-K. Kang, J. Cranford, M. K. Sridhar, D. Kodali, D. B. Landrum, and N. Slegers: AIAA J. **56** (2018) 15. https://doi.org/10.2514/1.J055360
25 J. A. Pohly, C. -K. Kang, T. K. C., T. Lee, and H. Aono: Proc. AIAA SciTech Forum (AIAA, 2023) 1–15.
26 M. Fuchiwaki, T. Kuroki, K. Tanaka, and T. Tabata: Exp. Fluids **54** (2013) 1. https://doi.org/10.1007/s00348-012-1450-x
27 Y. J. Lin, S. K. Lai, Y. H. Lai, and J. T. Yang: R. Soc. Open Sci. **8** (2021) 1. https://doi.org/10.1098/rsos.202172
28 R. Twigg, M. K. Sridhar, J. A. Pohly, N. Hilderbrant, C. K. Kang, D. B. Landrum, K. H. Roh, and S. Salzwedel: Proc. AIAA SciTech Forum 2020 (AIAA, 2020) 1–17.
29 M. K. Sridhar, J. A. Pohly, C. K. Kang, D. B. Landrum, T. Lee, and H. Aono: Proc. AIAA SciTech Forum 2021 (AIAA, 2021) 1–17.
30 K. Akama: Single-camera Model Deformation Measurement using a Data-driven Linear Reduced-order Model, Master's Thesis in Tohoku University (2020) pp. 1–49 (In Japanese).

About the Authors

Shogo Miyasaka received his B.S. degree from Shinshu University, Japan, in 2021. Since 2021, he has been a graduate student at the Department of Biomedical Engineering, Graduate School of Science and Technology, Shinshu University. His research interests are in butterfly flight and bio-inspired aerial robots. (21bs219e@shinshu-u.ac.jp)

Chang-kwon Kang received his B.S. and M.Sc. degrees from Delft University of Technology, Netherlands, in 2001 and 2005, respectively, and his Ph.D. degree from the University of Michigan, Ann Arbor, MI. From 2011 to 2013, he was a postdoctoral research fellow at the University of Michigan, Ann Arbor, MI. From 2013 to 2019, he was an assistant professor at the University of Alabama in Huntsville, AL. Since 2019, he has been an associate professor at the University of Alabama in Huntsville, AL. His research interests are in unsteady aerodynamics, bioinspired aerospace engineering, computational fluid dynamics, and fluid-structure interaction. (ck0025@uah.edu)

Hikaru Aono received his B.S., M.S. and Ph.D. degrees from Chiba University, Japan, in 2004, 2005, and 2008, respectively. From 2008 to 2011, he was a postdoctoral research fellow at the University of Michigan, Ann Arbor, MI. From 2011 to 2015, he was a research scientist at the Japan Aerospace Exploration Agency. From 2015 to 2020, he was an assistant professor at Tokyo University of Science, Japan. Since 2020, he has been an associate professor at Shinshu University. His research interests are in flapping-wing aerodynamics and robots, computational fluid dynamics, flight dynamics and control, and flow control. (aono@shinshu-u.ac.jp)